

# Monomeric and Dimeric Copper(II) Complexes of a Novel Tripodal Peptide Ligand: Structures Stabilized via Hydrogen Bonding or Ligand Sharing

John M. Rowland, Marilyn M. Olmstead, and Pradip K. Mascharak\*

Department of Chemistry and Biochemistry, University of California, Santa Cruz, California 95064, and Department of Chemistry, University of California, Davis, California 95616

Received May 1, 2000

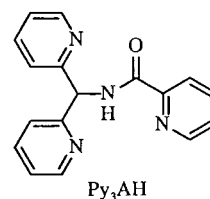
The novel tripodal ligand *N*-(bis(2-pyridyl)methyl)-2-pyridinecarboxamide (Py<sub>3</sub>AH) affords monomeric and dimeric copper(II) complexes with coordinated carboxamido nitrogens. Although many chloro-bridged dimeric copper(II) complexes are known, [Cu(Py<sub>3</sub>A)(Cl)] (**1**) remains monomeric and planar with a pendant pyridine and does not form either a chloro-bridged dimer or the ligand-shared dimeric complex [Cu(Py<sub>3</sub>A)(Cl)]<sub>2</sub> (**4**) in solvents such as CH<sub>3</sub>CN. When **1** is dissolved in alcohols, square pyramidal alcohol adducts [Cu(Py<sub>3</sub>A)(Cl)(CH<sub>3</sub>OH)] (**2**) and [Cu(Py<sub>3</sub>A)(Cl)(C<sub>2</sub>H<sub>5</sub>OH)] (**3**) are readily formed. In **2** and **3**, the ROH molecules are bound at axial site of copper(II) and the weak axial binding of the ROH molecule is strengthened by intramolecular hydrogen bonding between ROH and the pendant pyridine nitrogen. Two ligand-shared dimeric species [Cu(Py<sub>3</sub>A)(Cl)]<sub>2</sub> (**4**) and [Cu(Py<sub>3</sub>A)]<sub>2</sub>(ClO<sub>4</sub>)<sub>2</sub> (**5**) have also been synthesized in which the pendant pyridine of one [Cu(Py<sub>3</sub>A)] unit completes the coordination sphere of the other [Cu(Py<sub>3</sub>A)] neighbor. These ligand-shared dimers are obtained in aqueous solutions or in complete absence of chloride in the reaction mixtures.

## Introduction

Designed ligands with pendant donor groups have been utilized to synthesize ligand-shared dimeric copper(II) complexes.<sup>1–8</sup> In selected cases, the monomeric copper(II) complexes of these ligands have also been obtained under different reaction conditions.<sup>1,2,9</sup> When the disposition of the donor groups on a rigid ligand frame does not allow formation of a monomer, only the ligand-shared dimers are obtained.<sup>3–6</sup> Ligands with enough flexibility on the other hand can give rise to situations where both monomers and the corresponding ligand-shared dimer exist in equilibrium in the reaction mixtures.<sup>7</sup> Studies on monomer–dimer conversions could provide insights into the factors that dictate the process of ligand-sharing and allow formation of these species under specific reaction conditions.

For sometime, we have been interested in copper(II) com-

plexes with ligated carboxamido nitrogens.<sup>10–13</sup> To explore the chemistry of the 2-pyridinecarboxamide moiety, we have now synthesized a new ligand *N*-(bis(2-pyridyl)methyl)-2-pyridinecarboxamide (Py<sub>3</sub>AH; H represents the dissociable amide hydrogen). The design of this ligand is such that, in the



deprotonated form, Py<sub>3</sub>A<sup>−</sup> binds copper(II) center in a planar tridentate arrangement with two pyridine and one carboxamido nitrogens. Due to planarity of the N<sub>py</sub>–N<sub>carboxamido</sub>–N<sub>py</sub> moiety, one pyridine of the bis(pyridyl) unit fails to coordinate to the same copper(II) center, and we have utilized this fact to synthesize stable ligand-shared dimeric copper(II) complexes. In this paper, we report the syntheses, structures, and the spectroscopic properties of three monomeric and two ligand-shared dimeric copper(II) complexes of Py<sub>3</sub>AH. In two of these monomeric species, the ligand frame provides stability to ROH (R = Me, Et) molecules at the axial site of the copper(II) center via unique intramolecular hydrogen bonding between the pendant pyridine and axially bound ROH. The conditions under which these species interconvert into one another have also been identified. Solution studies demonstrate that the dimeric com-

\* To whom correspondence should be addressed at the University of California at Santa Cruz.

- (1) Kajikawa, Y.; Sakurai, T.; Azuma, N.; Kohno, S.; Tsuboyama, S.; Kobayashi, K.; Mukai, K.; Ishizu, K. *Bull. Chem. Soc. Jpn.* **1984**, 1454.
- (2) Brown, S. J.; Hudson, S. E.; Stephan, D. W.; Mascharak, P. K. *Inorg. Chem.* **1989**, 28, 468.
- (3) Koolhaas, G. J. A. A.; Driessen, W. L.; Reedijk, J.; Kooijman, H.; Spek, A. L. *J. Chem. Soc., Chem. Commun.* **1995**, 517.
- (4) Koolhaas, G. J. A. A.; Driessen, W. L.; Reedijk, J.; van der Plas, J. L.; de Graaff, R. A. G.; Gatteschi, D.; Kooijman, H.; Spek, A. L. *Inorg. Chem.* **1996**, 35, 1509.
- (5) Campbell, C. J.; Driessen, W. L.; Reedijk, J.; Smeetsand, W.; Spek, A. L. *J. Chem. Soc., Dalton Soc.* **1998**, 2703.
- (6) Xu, Z.; Thompson, L. K.; Matthews, C. J.; Miller, D. O.; Goeta, A. E.; Wilson, C.; Howard, J. A. K.; Ohba, M.; Okawa, H. *J. Chem. Soc., Dalton Trans.* **2000**, 69.
- (7) Comba, P.; Gavrish, S. P.; Lampeka, Y. D.; Peters, P. L. A. *J. Chem. Soc., Dalton Trans.* **1999**, 4099.
- (8) Fritsky, I. O.; Kozłowski, H.; Prisyazhnaya, E. V.; Rzaczyńska, Z.; Karaczyn, A.; Sliva, T. Y.; Glowiak, T. *J. Chem. Soc., Dalton Trans.* **1998**, 3629.
- (9) Duda, A. M.; Karaczyn, A.; Kozłowski, H.; Fritsky, I. O.; Glowiak, T.; Prisyazhnaya, E. V.; Sliva, T. Y.; Swiatek-Kozłowska, J. *J. Chem. Soc., Dalton Trans.* **1997**, 3853.

- (10) Brown, S. J.; Stephan, D. W.; Mascharak, P. K. *J. Am. Chem. Soc.* **1988**, 110, 1996.
- (11) Scheich, L. A.; Gosling, P.; Brown, S. J.; Olmstead, M. M.; Mascharak, P. K. *Inorg. Chem.* **1991**, 30, 1677.
- (12) Chavez, F. A.; Olmstead, M. M.; Mascharak, P. K. *Inorg. Chem.* **1996**, 35, 1410.
- (13) Chavez, F. A.; Olmstead, M. M.; Mascharak, P. K. *Inorg. Chim. Acta* **1998**, 269, 269.

plexes remain intact even at low concentrations while the monomeric complexes do not dimerize at high concentrations. It is thus clear that there is no equilibrium between monomer and dimer in any case; the desired form is obtained exclusively depending on the reaction conditions.

### Experimental Section

**Materials.** Copper(II) chloride dihydrate ( $\text{CuCl}_2 \cdot 2\text{H}_2\text{O}$ ), copper(II) perchlorate hexahydrate ( $\text{Cu}(\text{ClO}_4)_2 \cdot 6\text{H}_2\text{O}$ ), and 2-picolinic acid were purchased from Aldrich Chemical Co and were used without further purification. *N,N'*-dimethylformamide (DMF), acetonitrile ( $\text{CH}_3\text{CN}$ ), tetrahydrofuran (THF), and diethyl ether were distilled from  $\text{BaO}$ .  $\text{CaH}_2$ , Na/benzophenone, and metallic sodium, respectively. (Bis(2-pyridyl)-methyl)amine was synthesized by following a published procedure.<sup>14</sup> All the reported complexes afforded satisfactory elemental analyses (Atlantic Microlab Inc.).

**Preparation of Compounds.  $\text{Py}_3\text{AH}$ .** A solution of 3.061 g (16.5 mmol) of (bis(2-pyridyl)methyl)amine in 20 mL of THF was slowly added to a solution of 2.343 g (16.5 mmol) of 2-picolinic acid chloride and excess triethylamine (2.0 g) in 40 mL of THF at 0 °C. The resulting mixture was then warmed to 60 °C and heated for 20 min. Next it was cooled to 0 °C and filtered to remove  $\text{Et}_3\text{NHCl}$ . Removal of THF from the filtrate afforded crude  $\text{Py}_3\text{AH}$  as a cream-colored solid. This solid was dissolved in methylene chloride ( $\text{CH}_2\text{Cl}_2$ ) and washed with aqueous sodium hydroxide. The  $\text{CH}_2\text{Cl}_2$  layer was collected, and the solvent was removed in vacuo. Pure  $\text{Py}_3\text{AH}$  was obtained upon recrystallization of the residue from hot methanol. Yield: 80%.  $^1\text{H}$  NMR (303 K,  $\text{CDCl}_3$ , 250 MHz):  $\delta$  (ppm from TMS) 6.48 (d, 1H) 7.16 (t, 2H) 7.43 (t, 1H) 7.52 (d, 1H) 7.64 (t, 2H) 7.82 (t, 1H) 8.18 (d, 1H) 8.60 (d, 2H) 8.67 (d, 1H) 10.05 (d, 1H). Selected IR frequency (KBr disk):  $\nu_{\text{CO}}$  1666  $\text{cm}^{-1}$ .

**$[\text{Cu}(\text{Py}_3\text{A})(\text{Cl})]$  (1).** A batch of 0.02 g (0.84 mmol) of NaH was slowly added to a solution of 0.204 g (0.70 mmol) of  $\text{Py}_3\text{AH}$  dissolved in 40 mL of DMF. To this solution of the deprotonated ligand was then added with stirring a solution of 0.119 g (0.703 mmol) of  $\text{CuCl}_2 \cdot 2\text{H}_2\text{O}$  in 5 mL of DMF. After the reaction mixture was stirred for 1 h, the solvent was removed in vacuo. The resulting blue solid was redissolved in hot  $\text{CH}_3\text{CN}$ , and the solution was filtered to remove solid sodium chloride. The blue filtrate afforded dark blue crystals of **1** upon standing at room temperature. Yield: 38%. Selected IR frequencies (KBr disk,  $\text{cm}^{-1}$ ): 3060 (m), 1638 (s,  $\nu_{\text{CO}}$ ), 1621 (s), 1596 (s), 1560 (s), 1472 (s), 1431 (s), 1396 (s), 1044 (m), 1024 (m), 771 (s). Absorption spectrum in  $\text{CH}_3\text{CN}$ ,  $\lambda_{\text{max}}$ , nm ( $\epsilon$ ,  $\text{M}^{-1} \text{cm}^{-1}$ ): 620 (124), 290 sh (3 600), 265 (13 900).

**$[\text{Cu}(\text{Py}_3\text{A})(\text{Cl})(\text{CH}_3\text{OH})]$  (2).** A batch of 0.022 g (0.96 mmol) of metallic sodium was dissolved in 30 mL of methanol. A solution of 0.278 g (0.96 mmol) of  $\text{Py}_3\text{AH}$  in 10 mL of methanol was then added dropwise to the solution of sodium methoxide. Addition of a solution of 0.1631 g (0.958 mmol) of  $\text{CuCl}_2 \cdot 2\text{H}_2\text{O}$  in 10 mL of methanol to this solution of the deprotonated ligand resulted in a blue precipitate. The reaction mixture was then heated to obtain a clear blue solution. Blue crystals of complex **2** (yield 45%) separated from this solution upon standing at room temperature. Selected IR frequencies (KBr disk,  $\text{cm}^{-1}$ ): 3510 (br, s), 3200 (br, m), 1638 (s,  $\nu_{\text{CO}}$ ), 1628 (s), 1596 (s), 1568 (s), 1473 (m), 1385 (s), 1287 (m), 1025 (s), 760 (s), 697 (m). Absorption spectrum in  $\text{CH}_3\text{OH}$ ,  $\lambda_{\text{max}}$ , nm ( $\epsilon$ ,  $\text{M}^{-1} \text{cm}^{-1}$ ): 630 (117), 285 sh (5000), 265 (13 900).

Complex **2** was directly obtained from **1** upon recrystallization from warm methanol.

**$[\text{Cu}(\text{Py}_3\text{A})(\text{Cl})(\text{CH}_3\text{CH}_2\text{OH})]$  (3).** This complex was synthesized by following the procedure used to isolate complex **2** except for the fact that ethanol was used in place of methanol. Yield: 40%. Complex **3** was also obtained directly from **1** upon recrystallization from ethanol. Selected IR frequencies (KBr disk,  $\text{cm}^{-1}$ ): 3500 (br, m), 3180 (br, m), 1638 (s,  $\nu_{\text{CO}}$ ), 1628 (s), 1595 (s), 1568 (s), 1473 (m), 1388 (s), 1286 (m), 1084 (m), 1050 (m), 1025 (s), 762 (s), 699 (m). Absorption spectrum in  $\text{C}_2\text{H}_5\text{OH}$ ,  $\lambda_{\text{max}}$ , nm ( $\epsilon$ ,  $\text{M}^{-1} \text{cm}^{-1}$ ): 650 (133), 290 sh (5600), 265 (14 500).

**$[\text{Cu}(\text{Py}_3\text{A})(\text{Cl})_2 \cdot 8\text{H}_2\text{O}$  (4-8 $\text{H}_2\text{O}$ ).** A batch of 50 mg of complex **1** was placed in 5 mL of  $\text{CH}_3\text{CN}$  and the mixture was warmed to 50 °C, and to it a few drops of water were added to obtain a clear solution. Large crystals of **4** were obtained when this clear blue solution was stored at room temperature for 2 h. Yield: 35%. Selected IR frequencies (KBr disk,  $\text{cm}^{-1}$ ): 3400 (br, vs), 3065 (m), 1624 (s,  $\nu_{\text{CO}}$ ), 1598 (s), 1568 (s), 1478 (m), 1438 (m), 1396 (s), 1283 (m), 1027 (m), 762 (s), 700 (m), 603 (m). Absorption spectrum in water,  $\lambda_{\text{max}}$ , nm ( $\epsilon$ ,  $\text{M}^{-1} \text{cm}^{-1}$ ): 600 (125), 265 (14 800).

**$[\text{Cu}(\text{Py}_3\text{A})_2(\text{ClO}_4)_2 \cdot \text{CH}_3\text{CN} \cdot \text{H}_2\text{O}$  (5- $\text{CH}_3\text{CN} \cdot \text{H}_2\text{O}$ ).** A batch of 0.014 g (0.58 mmol) of NaH was added to a solution of 0.145 g (0.5 mmol) of  $\text{Py}_3\text{AH}$  in 40 mL of DMF. To this solution of the deprotonated ligand was added with stirring a solution of 0.185 g (0.5 mmol) of  $\text{Cu}(\text{ClO}_4)_2 \cdot 6\text{H}_2\text{O}$  in 5 mL of DMF. After 1 h of stirring, DMF was removed in vacuo and the blue residue was dissolved in 10 mL of  $\text{CH}_3\text{CN}$ . Diffusion of diethyl ether into the blue solution afforded dark blue crystals of **5** in 45% yield. Selected IR frequencies (KBr disk,  $\text{cm}^{-1}$ ): 3440 (br, s), 3073 (w), 1635 (s,  $\nu_{\text{CO}}$ ), 1605 (s), 1570 (s), 1476 (m), 1438 (m), 1388 (s), 1090 (vs,  $\nu_{\text{ClO}_4}$ ), 763 (s), 700 (m), 625 (s). Absorption spectrum in water,  $\lambda_{\text{max}}$ , nm ( $\epsilon$ ,  $\text{M}^{-1} \text{cm}^{-1}$ ): 600 (125), 265 (15 000).

**X-ray Data Collection and Structure Solution and Refinement.** Crystals suitable for X-ray analysis were obtained as follows: complex **1**, recrystallization from hot  $\text{CH}_3\text{CN}$ ; complex **2**, crystallization from concentrated  $\text{CH}_3\text{OH}$  solution; complex **3**, crystallization from concentrated EtOH solution; complex **4**  $\cdot 8\text{H}_2\text{O}$ , crystallization from aqueous  $\text{CH}_3\text{CN}$ ; complex **5**  $\cdot \text{CH}_3\text{CN} \cdot \text{H}_2\text{O}$ , diffusion of diethyl ether into solution of the complex in  $\text{CH}_3\text{CN}$ . Diffraction experiments were performed with a Bruker SMART 1000 system, and data were collected at 90 K.  $\text{Mo K}\alpha$  (0.710 73 Å) radiation was used, and the data were corrected for absorption. Intensities of two standard reflections showed only random fluctuations of less than 1% during the course of data collection. The structures were solved by using the standard SHELXS-97 package. Machine parameters, crystal data, and data collection parameters are summarized in Table 1. Selected bond distances and angles are listed in Table 2. Complete crystallographic data for the five complexes have been submitted as Supporting Information.

**Other Physical Measurements.** Absorption spectra were recorded on a Perkin-Elmer Lambda 9 spectrophotometer. A Perkin-Elmer 1600 FTIR spectrophotometer was used to monitor the infrared (IR) spectra. EPR spectra at X-band frequencies were obtained with a Bruker ESP-300 spectrometer.

### Results and Discussion

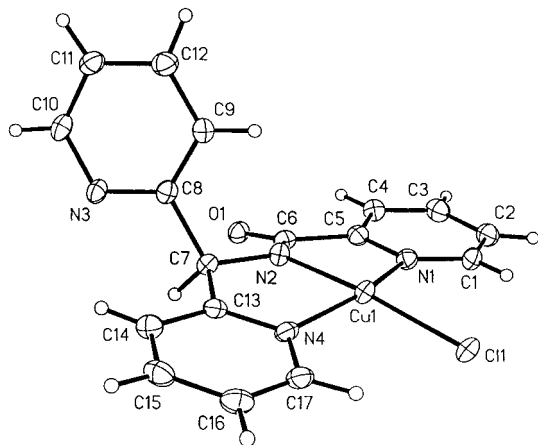
The deprotonated ligand  $\text{Py}_3\text{A}^-$  provides a somewhat rigid scaffolding around copper(II) ions due to the fact that deprotonation of the amide nitrogen makes a major portion of the ligand planar. The planar portion of  $\text{Py}_3\text{A}^-$  acts as a tridentate ligand consisting of two pyridine nitrogen and one carboxamido nitrogen donor. This mode of coordination by  $\text{Py}_3\text{A}^-$  does not allow coordination of the third pyridine nitrogen to the same copper(II) ion and results in monomeric complexes such as **1** with a pendant pyridine ring which could be used for further coordination. In the present work, we have observed another unusual behavior of this uncoordinated pyridine namely, stabilizing weakly bound axial alcohols via hydrogen bonding (complexes **2** and **3**).

In nonaqueous media, only monomeric complexes are formed with  $\text{Py}_3\text{A}^-$  when copper(II) chloride is used as the starting copper salt. The presence of  $\text{Cl}^-$  at the fourth site in the basal plane apparently prevents dimerization of the  $[\text{Cu}(\text{Py}_3\text{A})]$  units. No chloro-bridged dimer is obtained in any case. Dimerization of the  $[\text{Cu}(\text{Py}_3\text{A})]$  units via ligand-sharing however occurs when one provides means for chloride dissociation. Addition of water allows such dissociation of chloride ion, and one obtains the ligand-shared dimer **4** in which the pendant pyridine rings of two  $[\text{Cu}(\text{Py}_3\text{A})]$  units take part in ligation. Interestingly, the dissociated chloride ions come back and bind at axial sites of

**Table 1.** Summary of Crystal Data and Intensity and Structure Refinement Parameters for [Cu(Py<sub>3</sub>A)Cl] (**1**), [Cu(Py<sub>3</sub>A)(Cl)(CH<sub>3</sub>OH)] (**2**), [Cu(Py<sub>3</sub>A)(Cl)(C<sub>2</sub>H<sub>5</sub>OH)] (**3**), [Cu(Py<sub>3</sub>A)(Cl)]<sub>2</sub>·8H<sub>2</sub>O (**4**·8H<sub>2</sub>O), and [Cu(Py<sub>3</sub>A)]<sub>2</sub>(ClO<sub>4</sub>)<sub>2</sub>·CH<sub>3</sub>CN·H<sub>2</sub>O (**5**·CH<sub>3</sub>CN·H<sub>2</sub>O)

	complex				
	<b>1</b>	<b>2</b>	<b>3</b>	<b>4</b> ·8H <sub>2</sub> O	<b>5</b> ·CH <sub>3</sub> CN·H <sub>2</sub> O
formula	C <sub>17</sub> H <sub>13</sub> ClCu N <sub>4</sub> O	C <sub>18</sub> H <sub>17</sub> ClCu N <sub>4</sub> O <sub>2</sub>	C <sub>19</sub> H <sub>19</sub> ClCu N <sub>4</sub> O <sub>2</sub>	C <sub>34</sub> H <sub>42</sub> Cl <sub>2</sub> Cu <sub>2</sub> N <sub>8</sub> O <sub>10</sub>	C <sub>36</sub> H <sub>31</sub> Cl <sub>2</sub> Cu <sub>2</sub> N <sub>9</sub> O <sub>11</sub>
mol wt	388.30	420.35	434.37	920.74	963.68
cryst color, habit	blue needle	blue plate	blue block	blue needle	blue parallelepiped
<i>T</i> , K	90(2)	90(2)	89(2)	90(2)	89(2)
cryst system	monoclinic	monoclinic	monoclinic	monoclinic	triclinic
space group	<i>P</i> 2 <sub>1</sub> / <i>c</i>	<i>P</i> 2 <sub>1</sub> / <i>c</i>	<i>C</i> <i>c</i>	<i>C</i> 2/ <i>c</i>	<i>P</i> 1
<i>a</i> , Å	5.1467(3)	7.6942(5)	7.7803(4)	15.6008(6)	9.9838(5)
<i>b</i> , Å	10.6371(5)	28.550(2)	28.4159(15)	14.6822(6)	10.5102(5)
<i>c</i> , Å	28.3041(15)	8.2252(5)	8.4852(5)	17.6842(7)	18.2512(8)
$\alpha$ , deg	90	90	90	90	99.2660(10)
$\beta$ , deg	90.9930(10)	103.2210(10)	103.3910(10)	104.2610(10)	97.0640(10)
$\gamma$ , deg	90	90	90	90	92.6980(10)
<i>V</i> , Å <sup>3</sup>	1549.30(14)	1758.9(2)	1824.94(17)	3925.8(3)	1871.42(15)
<i>Z</i>	4	4	4	4	2
<i>d</i> <sub>calcd</sub> , g cm <sup>-3</sup>	1.665	1.587	1.581	1.558	1.710
abs coef, $\mu$ , mm <sup>-1</sup>	1.594	1.414	1.366	1.285	1.355
GOF <sup>a</sup> on <i>F</i> <sup>2</sup>	0.880	1.029	1.143	0.930	0.993
<i>R</i> <sub>1</sub> , <sup>b</sup> %	4.37	3.40	2.73	3.55	4.17
<i>R</i> <sub>w2</sub> , <sup>c</sup> %	9.20	7.91	6.25	7.80	10.93

<sup>a</sup> GOF =  $[\sum[w(F_o^2 - F_c^2)^2]/(M - N)]^{1/2}$  (*M* = number of reflections, *N* = number of parameters refined). <sup>b</sup> *R*<sub>1</sub> =  $\sum||F_o| - |F_c||/\sum|F_o|$ . <sup>c</sup> *R*<sub>w2</sub> =  $[\sum[w(F_o^2 - F_c^2)^2]/\sum[w(F_o^2)^2]]^{1/2}$ .

**Figure 1.** Thermal ellipsoid (probability level 50%) plot of [Cu(Py<sub>3</sub>A)Cl] (**1**) with the atom-labeling scheme.

the [Cu(Py<sub>3</sub>A)]<sub>2</sub> unit to generate complex **4**. The dimeric complex **4** easily converts back to monomeric complex **1** when warmed in CH<sub>3</sub>CN. Since the chloride ion occupies an equatorial position in **1**, it appears that (a) the reversible **1** ↔ **4** conversion requires dissociation and religation of chloride ion and (b) complex **1** is the stable species in CH<sub>3</sub>CN. Since dissociation of chloride ion is not favored in CH<sub>3</sub>CN and alcohols, one obtains only monomeric species **1**–**3**. In complexes **2** and **3**, axial ROH ligands are hydrogen bonded by the pendant pyridine. The synthesis of the dimeric complex **5** directly from copper(II) perchlorate confirms the role of chloride ion preventing dimer formation in the case of **1**–**3**.

**Structure of [Cu(Py<sub>3</sub>A)Cl] (**1**).** The structure of complex **1** consists of monomeric [Cu(Py<sub>3</sub>A)Cl] units (Figure 1). The copper(II) center exists in a slightly distorted square planar geometry with Py<sub>3</sub>A<sup>-</sup> acting as a tridentate ligand. A chloride ion, trans to the carboxamido nitrogen, completes coordination in the square plane. The rigidity of the planar N<sub>py</sub>–N<sup>-</sup><sub>amido</sub>–N<sub>py</sub> backbone of Py<sub>3</sub>A<sup>-</sup> does not allow coordination of the third pyridine ring to the copper(II) center, and it remains uncoordinated but ordered in the crystal lattice. The Cu(II)–N<sub>amido</sub> and Cu(II)–N<sub>py</sub> distances in **1** (1.914(2) and 2.014(2) Å, respec-

tively) are comparable to analogous distances in other known complexes.<sup>10,12,13</sup> Considerable strain exists in the coordination plane around the copper(II) center due to the short bite (160°) of the N<sub>py</sub>–N<sup>-</sup><sub>amido</sub>–N<sub>py</sub> portion of the Py<sub>3</sub>A<sup>-</sup> ligand frame.

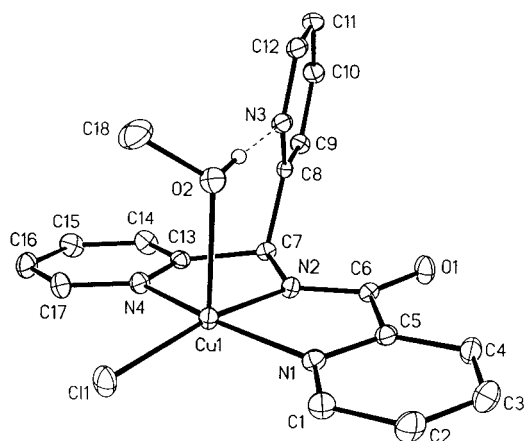
In solid state, the monomeric units of **1** are arranged in a chain-like fashion (Figure S1, Supporting Information) such that the coordinated chloride of one monomeric unit stacks on the next one to axially interact with the neighboring copper(II) center. The Cu(II)···Cl distance is however long (3.9965(9) Å) and indicates very weak interaction. This distance is significantly longer than Cu(II)–Cl distance of 2.831(1) Å observed in a true chloride-bridged dimer of similar ligand.<sup>15</sup> The carbonyl oxygens are also involved in weak axial interaction (Cu(II)–O = 2.533(2) Å) in this chain structure (Figure S1). These weak axial interactions between copper(II) monomers are absent in solutions of **1** as evidenced by EPR spectroscopy (vide infra). Interestingly, copper(II) complexes of similar ligands with N<sub>py</sub>–N<sub>amido</sub>–N<sub>imidazole</sub> moiety have been found to exist either as chloro-bridged dimer or chloro-bridged infinite chain.<sup>15</sup>

**Structure of [Cu(Py<sub>3</sub>A)(Cl)(CH<sub>3</sub>OH)] (**2**).** The structure **2** is shown in Figure 2. The copper(II) center is in a square pyramidal geometry with the apical position occupied by a molecule of methanol. Comparison of **1** and **2** reveals similar mode of coordination by the Py<sub>3</sub>A<sup>-</sup> ligand and chloride in the basal plane of copper. Interestingly, the coordination of methanol is stabilized by an intramolecular hydrogen bond between the methanolic hydrogen and the nitrogen of the noncoordinating pyridine. The copper(II)–CH<sub>3</sub>OH distance is 2.3297(14) Å. Although methanol is not a good ligand, metal-bound methanol(s) has been observed in metal complexes with solvated cavities stabilized by hydrogen bonding.<sup>16–19</sup> In the present case, only the pendant pyridine from the Py<sub>3</sub>A<sup>-</sup> ligand assists binding of

- (15) Brown, S. J.; Tao, X.; Wark, T. A.; Stephan, D. W.; Mascharak, P. K. *Inorg. Chem.* **1988**, *27*, 1581.  
 (16) Walton, P. H.; Boxwell, C. J. *J. Chem. Soc., Chem. Commun.* **1999**, 1647.  
 (17) Cronin, L.; Greener, B.; Moore, M. H.; Walton, P. H. *J. Chem. Soc., Dalton Trans.* **1996**, 3337.  
 (18) Goodgame, D. M.; Hill, S. P. W.; Smith, A. M.; Williams, D. J. *J. Chem. Soc., Dalton Trans.* **1994**, 859.  
 (19) Barkigia, K. M.; Berber, M. D.; Fajer, J.; Medforth, C. J.; Renner, M. W.; Smith, K. M. *J. Am. Chem. Soc.* **1990**, *112*, 8851.

**Table 2.** Selected Bond Distances (Å) and Angles (deg)

Complex 1				Complex 48H <sub>2</sub> O			
Cu—N1	2.028(2)	N2—C7	1.451(4)	Cu1—N1	2.0205(15)	N1—C5	1.356(2)
Cu—N2	1.914(2)	N4—C13	1.324(4)	Cu1—N2	1.9209(15)	N2—C6	1.324(2)
Cu—N4	2.014(2)	N4—C17	1.359(4)	Cu1—N4	2.0187(16)	N2—C7	1.456(2)
Cu—Cl1	2.2312(8)	C5—C6	1.511(4)	Cu1—Cl1	2.7029(5)	C7—C8	1.525(2)
N1—C1	1.331(4)	O1—C6	1.246(3)	Cu1—N3A	2.0139(15)	N4—C17	1.347(2)
N1—C5	1.347(4)	Cu—O1#1	2.533(2)	Cu1—Cu1A	3.2235(4)	C5—C6	1.507(2)
N2—C6	1.323(4)	Cu—Cl1#2	3.9965(9)	N1—C1	1.338(2)	O1—C6	1.246(2)
N1—Cu—Cl1	97.29(7)	Cu—N1—C5	111.65(19)	N1—Cu1—Cl1	83.58(4)	N3A—Cu1—Cl1	100.13(4)
N1—Cu—N2	81.63(10)	Cu—N2—C6	118.2(2)	N1—Cu1—N2	81.82(6)	Cu1—N1—C5	111.69(112)
N1—Cu—N4	160.28(10)	Cu—N4—C13	115.21(19)	N1—Cu1—N4	161.83(6)	Cu1—N2—C6	117.31(12)
N2—Cu—Cl1	173.44(8)	N2—C6—C5	111.0(3)	N1—Cu1—N3A	100.62(6)	Cu1—N4—C13	114.93(12)
N2—Cu—N4	82.22(10)	N2—C6—O1	128.1(3)	N2—Cu1—Cl1	96.53(5)	Cu1A—N3—C8	123.35(12)
N4—Cu—Cl1	98.64(7)	C5—C6—O1	120.9(3)	N2—Cu1—N4	81.32(6)	N2—C6—C5	112.07(15)
Complex 2				Complex 5·CH <sub>3</sub> CN·H <sub>2</sub> O			
Cu—N1	2.0316(14)	N2—C6	1.331(2)	Cu1—N1	2.036(2)	N4—C17	1.347(3)
Cu—N2	1.9223(15)	N2—C7	1.451(2)	Cu1—N2	1.9079(19)	N5—C18	1.343(3)
Cu—N4	2.0278(14)	N4—C13	1.337(2)	Cu1—N4	2.014(2)	N5—C22	1.353(3)
Cu—Cl1	2.2253(5)	N4—C17	1.353(2)	Cu1—N7	2.003(2)	N6—C23	1.331(3)
Cu—O2	2.3297(14)	C5—C6	1.518(2)	Cu1—Cu2	3.0943(4)	N7—C25	1.351(3)
N1—C1	1.340(2)	O1—C6	1.254(2)	N1—C1	1.344(3)	N8—C30	1.349(3)
N1—C5	1.355(2)	O2—H2A	0.877(17)	N1—C5	1.358(3)	C5—C6	1.510(3)
N1—Cu—Cl1	98.16(4)	Cl1—Cu—O2	101.55(4)	N2—C6	1.335(3)	C6—O1	1.239(3)
N1—Cu—N2	80.92(6)	Cu—N1—C5	112.45(11)	N2—C7	1.453(3)	C22—C23	1.515(3)
N1—Cu—N4	160.80(6)	Cu—N2—C6	119.86(12)	N3—C8	1.351(3)	C23—O2	1.244(3)
N1—Cu—O2	93.78(5)	Cu—N4—C13	114.71(11)	N1—Cu1—N2	82.29(8)	Cu2—N3—C8	121.84(16)
N2—Cu—Cl1	169.63(5)	Cu—O2—C18	121.98(14)	N1—Cu1—N4	160.87(8)	Cu2—N5—C22	111.45(17)
N2—Cu—N4	81.08(6)	Cu—O2—H2A	102(2)	N1—Cu1—N7	99.24(8)	Cu2—N6—C23	118.7(2)
N2—Cu—O2	88.83(6)	N2—C6—C5	110.60(15)	N2—Cu1—N4	81.41(8)	Cu2—N8—C30	14.77(16)
N4—Cu—Cl1	98.34(4)	N2—C6—O1	128.34(16)	N2—Cu1—N7	166.16(8)	N2—C6—C5	111.9(2)
N4—Cu—O2	92.47(5)	C5—C6—O1	121.04(15)	N4—Cu1—N7	98.98(8)	N2—C6—O1	127.4(2)
Complex 3				Complex 5·CH <sub>3</sub> CN·H <sub>2</sub> O			
Cu—N1	2.0359(18)	N2—C6	1.323(2)	Cu1—N1	2.036(2)	N4—C17	1.347(3)
Cu—N2	1.9289(15)	N2—C7	1.444(2)	Cu1—N2	1.9079(19)	N5—C18	1.343(3)
Cu—N4	2.0323(18)	N4—C13	1.345(3)	Cu1—N4	2.014(2)	N5—C22	1.353(3)
Cu—Cl1	2.2260(5)	C18—C19	1.512(3)	Cu1—N7	2.003(2)	N6—C23	1.331(3)
Cu—O2	2.3182(14)	C5—C6	1.518(3)	Cu1—Cu2	3.0943(4)	N7—C25	1.351(3)
N1—C1	1.344(3)	O1—C6	1.249(2)	N1—C1	1.344(3)	N8—C30	1.349(3)
O2—C18	1.436(2)	O2—H2A	0.822(17)	N1—C5	1.358(3)	C5—C6	1.510(3)
N1—Cu—Cl1	98.21(5)	Cl1—Cu—O2	99.13(4)	N2—C6	1.335(3)	C6—O1	1.239(3)
N1—Cu—N2	80.68(7)	Cu—N1—C5	112.38(14)	N2—C7	1.453(3)	C22—C23	1.515(3)
N1—Cu—N4	157.72(6)	Cu—N2—C6	119.38(13)	N3—C8	1.351(3)	C23—O2	1.244(3)
N1—Cu—O2	91.61(6)	Cu—N4—C13	114.90(14)	N1—Cu1—N2	82.29(8)	Cu2—N3—C8	121.84(16)
N2—Cu—Cl1	173.30(5)	Cu—O2—C18	128.45(13)	N1—Cu1—N4	160.87(8)	Cu2—N5—C22	111.45(17)
N2—Cu—N4	80.80(7)	Cu—O2—H2A	99(2)	N1—Cu1—N7	99.24(8)	Cu2—N6—C23	118.7(2)
N2—Cu—O2	87.52(6)	N2—C6—C5	111.06(16)	N2—Cu1—N4	81.41(8)	Cu2—N8—C30	14.77(16)
N4—Cu—Cl1	98.73(5)	N2—C6—O1	128.01(17)	N2—Cu1—N7	166.16(8)	N2—C6—C5	111.9(2)
N4—Cu—O2	99.86(6)	C5—C6—O1	120.91(17)	N4—Cu1—N7	98.98(8)	N2—C6—O1	127.4(2)
				N5—Cu—N6	81.87(9)	N2—C7—C8	112.24(19)
				N5—Cu—N3	98.39(9)	C5—C6—O1	120.7(2)
				N6—Cu—N8	160.45(9)	N6—C23—C22	111.7(2)
				Cu1—N1—C5	130.08(17)	N6—C23—O2	127.3(2)
				Cu1—N2—C6	118.13(16)	N6—C24—C25	113.12(19)
				Cu1—N4—C13	115.10(16)	C22—C23—O2	121.0(2)

**Figure 2.** Thermal ellipsoid (probability level 50%) plot of [Cu(Py<sub>3</sub>A)(Cl)(CH<sub>3</sub>OH)] (**2**) with the atom-labeling scheme. H atoms are omitted for the sake of clarity. Hydrogen bonding between the axially coordinated methanol molecule and the nitrogen of the pendant pyridine ring is indicated.

methanol at the axial site of copper and no lattice solvent molecule(s) is involved in hydrogen bonding. In this regard,

the structure of **2** (and **3**; vide infra) is somewhat unusual.<sup>20</sup> The crystal structure of **2** does not contain any other axial interaction(s) between neighboring units as those seen in the lattice structure of complex **1**.

**Structure of [Cu(Py<sub>3</sub>A)(Cl)(CH<sub>3</sub>CH<sub>2</sub>OH)] (**3**).** The crystal structure of **3** is shown in Figure 3. The coordination geometry around copper(II) in this complex is very similar to that in **2**; the only difference is the presence of an ethanol molecule at the apical position. Here also, the pendant pyridine of the Py<sub>3</sub>A<sup>−</sup> ligand is H-bonded to the alcohol and the Cu(II)—C<sub>2</sub>H<sub>5</sub>OH distance (2.3182(14) Å) is very similar to the Cu(II)—CH<sub>3</sub>OH distance found in **2**. In copper(II) complexes with ethanol as ligands in the equatorial plane, Cu(II)—C<sub>2</sub>H<sub>5</sub>OH distances are much shorter (2.04–2.07 Å).<sup>21</sup> Successful isolation of **2** and **3**

(20) The 2,2'-bipyridine-*N,N'*-dioxide complex [Cu(bpyO<sub>2</sub>)(MeOH)Cl<sub>2</sub>] contains a methanol molecule as ligand that is not H-bonded to any solvent molecule. The methanol molecule occupies an equatorial position, and the Cu(II)—CH<sub>3</sub>OH distance is considerably short (1.98 Å). See: Koman, M.; Baran, P.; Valigura, D. *Acta Crystallogr.* **1991**, *C47*, 2529.

(21) Martens, C. F.; Schenning, A. P. H. J.; Feiters, M. C.; Berens, H. W.; van der Linden, J. G. M.; Admiraal, G.; Beurskens, P. T.; Kooijman, H.; Spek, A. L.; Nolte, R. J. M. *Inorg. Chem.* **1995**, *34*, 4735.

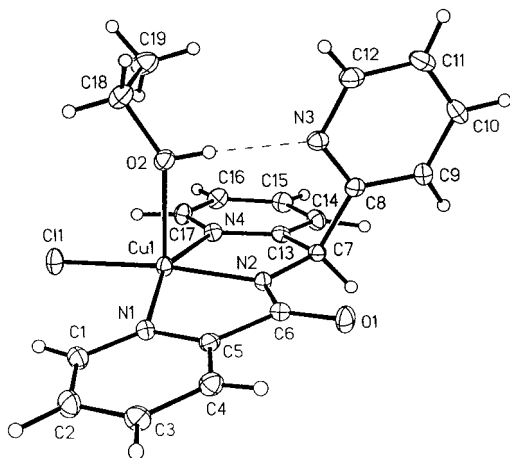


**Figure 3.** Thermal ellipsoid (probability level 50%) plot of  $[\text{Cu}(\text{Py}_3\text{A})(\text{Cl})(\text{C}_2\text{H}_5\text{OH})]$  (**3**) with the atom-labeling scheme. Hydrogen bonding between the axially coordinated ethanol molecule and the nitrogen of the pendant pyridine ring is indicated.

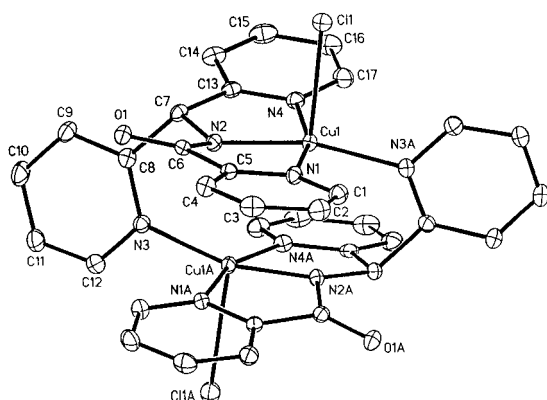


**Figure 4.** Thermal ellipsoid (probability level 50%) plot of  $[\text{Cu}(\text{Py}_3\text{A})(\text{Cl})]_2$  (**4**) with the atom-labeling scheme. H atoms and the lattice water molecules are omitted for the sake of clarity.

indicates that intramolecular hydrogen bonding by the pendant pyridine in  $[\text{Cu}(\text{Py}_3\text{A})\text{Cl}]$  is the key for the ligation of alcohols at the axial position of the copper(II) center. This is especially notable since one otherwise expects very poor interaction between alcohols (weak ligands) and the Jahn–Teller sensitive copper(II) center. It is also important to note that formation of such alcohol adducts precedes the other possibilities of formation of chloride-bridged dimer or chain. The  $\text{N}(3)\text{—O}(2)$  distances in **2** and **3** (2.840(2) and 2.834(2) Å, respectively) indicate considerably strong hydrogen-bonding interaction between the pendant pyridine nitrogen and the alcohol molecules.<sup>22</sup>

**Structure of  $[\text{Cu}(\text{Py}_3\text{A})(\text{Cl})]_2 \cdot 8\text{H}_2\text{O}$  (**4**).** The structure of the dimeric complex **4** without the water molecules is shown in Figure 4. Each copper(II) center exists in slightly distorted square pyramidal geometry with equatorial ligation by the pendant pyridine arm of a second copper(II) monomer. The mode of ligand sharing by the bis(2-pyridine) unit of  $\text{Py}_3\text{A}^-$  is similar to that noted with a ligand with bis(2-imidazole) moiety which facilitates formation of ligand-shared copper(II) dimer.<sup>3,4</sup> In **4**, the  $\text{N}_{\text{py}}\text{—N}_{\text{amido}}\text{—N}_{\text{py}}$  moiety of the  $\text{Py}_3\text{A}^-$  ligand is also planar and maintains an angle of 161.83(6)° at the copper(II) center. Two chloride ions occupy the outer axial sites of the two copper centers. The copper(II)— $\text{N}_{\text{amido}}$  distance (1.9209(15) Å) in **4** is similar to those found complexes **1–3** despite the change in the nature of the trans ligand (chloride in

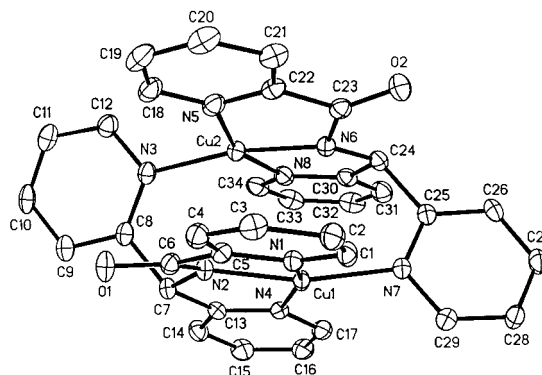
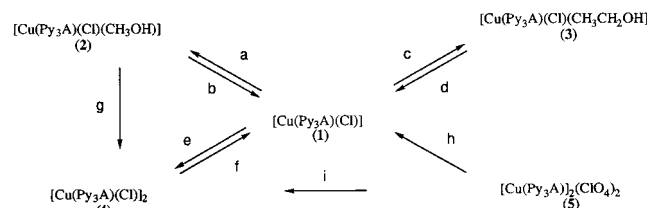


**Figure 5.** Thermal ellipsoid (probability level 50%) plot of the cation of  $[\text{Cu}(\text{Py}_3\text{A})]_2(\text{ClO}_4)_2$  (**5**) with the atom-labeling scheme. H atoms and the lattice solvent molecules are omitted for the sake of clarity.

### Scheme 1. Interconversion of **1–5**



**1–3** to pyridine in **4**). Weak ligation by the axial chlorides is indicated by the  $\text{Cu}(\text{II})\text{—Cl}$  distance of 2.7029(5) Å.

Dimerization of the  $[\text{Cu}(\text{Py}_3\text{A})]$  units introduces significant strain in **4** as evidenced by the short  $\text{N}2\text{—Cu}1\text{—N}3\text{A}$  angle (163.33(6)°, Figure 4). This strain is presumably responsible for the easy conversion of **4** back to **1** when one attempts to recrystallize **4** from  $\text{CH}_3\text{CN}$ . The 8 molecules of water are well-ordered between pyridine rings of adjacent dimers and exist as a H-bonded sheet of water molecules (Figure S2, Supporting Information). A small extent of  $\pi\text{—}\pi$  stacking between pyridine rings is noted in **4**, a fact that could provide some stability to the dimeric structure. The copper(II)—copper(II) distance in **4** is 3.223(4) Å, and the copper centers are not exactly coaxial (Figure 4).

**Structure of  $[\text{Cu}(\text{Py}_3\text{A})]_2(\text{ClO}_4)_2 \cdot \text{CH}_3\text{CN} \cdot \text{H}_2\text{O}$  (**5**).** The crystal structure of the cation of complex **5** is shown in Figure 5. The dimeric complex is structurally very similar to complex **4** except for the missing chloride ions at the outer axial sites on copper. There is weak axial interaction between the copper(II) centers and the oxygens of the perchlorate anions (average  $\text{Cu—O}(\text{perchlorate})$  distance 2.55 Å) in the structure of **5**. The copper(II)—copper(II) distance in **5** is 3.0943(4) Å, and the copper centers are also not coaxial (Figure 5). Overall, the dimeric  $[\text{Cu}(\text{Py}_3\text{A})]_2$  unit of **5** is slightly more compact compared to that in **4** (Table 2). For example, the copper(II)— $\text{N}_{\text{amido}}$  distances (1.9079(19) and 1.913(2) Å) are shorter than the same distance noted for **4** (1.9209(15) Å). There is no interaction between the dimeric cation and the water molecule in the crystal lattice.

**Interconversions of Complexes **1–5**.** Complexes **1–5** readily interconvert into one another. The interconversions of **1–5** are schematically shown in Scheme 1. To begin with, isolation of **1** is itself interesting since the reaction conditions do not afford the dimeric complex **4** or a chloro-bridged dimer as observed with complexes of similar ligands. When **1** is recrystallized from methanol, **2** (step a) is obtained. Complex **2** can also be obtained directly from addition of  $\text{CuCl}_2 \cdot 2\text{H}_2\text{O}$  to deprotonated  $\text{Py}_3\text{A}^-$  in methanol. When complex **2** is dried

under vacuum and the residue is recrystallized from hot  $\text{CH}_3\text{CN}$ , one obtains complex **1** (step b). Similarly, crystallization of **1** from ethanol affords **3** (step c) and recrystallization of a sample of dried **3** from hot  $\text{CH}_3\text{CN}$  results in formation of **1** (step d). The possibility of axial ligation of protic solvent molecules to the copper(II) center of **1** via hydrogen bonding with the pendant pyridine prompted us to try to isolate the water adduct of **1**. It was however surprising that addition of a small amount of water to  $\text{CH}_3\text{CN}$  solutions of **1** gave rise to crystalline **4** (step e). The dimerization of **1** is fast and can be followed by electronic absorption spectroscopy. Addition of water brings about a rapid shift of  $\lambda_{\text{max}}$  from 620 nm (for **1**) to 600 nm (for **4**). This dimerization process is also reversible. When **4** is thoroughly dried and recrystallized from hot  $\text{CH}_3\text{CN}$ , complex **1** is obtained in high yield (step f). It is important to note that the formation of **4** from **1** requires water and **4** cannot be recrystallized from neat  $\text{CH}_3\text{CN}$ . These observations clearly indicate that presence of water is essential for the dimerization of **1**. Quite in line with this conclusion, methanolic solutions of **1** also affords **4** (and not **2**) upon addition of small amounts of water (step g). Structural data for **1** and **4** reveal that significant rearrangement occurs upon conversion of **1** into **4**. The most noticeable one is the exchange of the position of the chloride ion from equatorial in **1** to axial in **4**. This process requires dissociation of chloride ion from **1** and religation at the axial sites in **4**. Since **1** can only be converted into **4** in the presence of water, it appears that water assists such dissociation of chloride from **1** and helps in formation of the dimeric species.

Under chloride-free conditions, reaction of  $\text{Py}_3\text{A}^-$  with  $\text{Cu}(\text{ClO}_4)_2 \cdot 6\text{H}_2\text{O}$  in  $\text{CH}_3\text{CN}$  affords the dimeric complex **5**. When **5** is thoroughly dried and recrystallized from hot  $\text{CH}_3\text{CN}$ , one gets back **5** (not a monomeric solvated species) in quantitative yield. It is therefore evident that  $\text{Py}_3\text{A}^-$  will afford dimeric species in  $\text{CH}_3\text{CN}$  if no chloride is present. However, in the presence of chloride, only monomeric **1** is obtained in  $\text{CH}_3\text{CN}$  (step h). This leads to the conclusion that chloride resists dimer formation in  $\text{CH}_3\text{CN}$ . Support to this conclusion comes from the fact that when **5** is dissolved in warm  $\text{CH}_3\text{CN}$  followed by the addition of excess  $\text{Et}_4\text{NCl}$ , blue crystals of **1** are formed within minutes (step h).

When **5** is warmed in 9:1 (v/v)  $\text{CH}_3\text{CN}:\text{H}_2\text{O}$  mixture with 4 equiv of  $\text{NaCl}$ , pure **4** is obtained in quantitative yield (step i). Axial coordination by chloride to the ligand-shared dimer **5** affords **4** in this step, and since the dimeric complex is stable in aqueous  $\text{CH}_3\text{CN}$ , it does not break apart to form **1**.

**Spectral Properties.** Coordination of carboxamido nitrogen to copper(II) in complexes **1–3** is evident from shift of the carbonyl stretching frequency ( $\nu_{\text{CO}}$ ) from 1670 to 1638  $\text{cm}^{-1}$ . In the dimeric species **4** and **5**,  $\nu_{\text{CO}}$  is noted at 1624  $\text{cm}^{-1}$ . The coordinated  $\text{MeOH}$  in **2** gives rise to a strong band at 1026  $\text{cm}^{-1}$  in addition to  $\nu_{\text{OH}}$  at 3150  $\text{cm}^{-1}$ . In **3**, the corresponding peaks for coordinated ethanol appears at 1050 and 3180  $\text{cm}^{-1}$ . The blue color for these species arises from a broad d–d band in the 580–620 nm region.

The monomeric complexes **1–3** exhibit axial EPR spectra typical for monomeric tetragonal copper(II) species with  $d_{x^2-y^2}$  ground-state doublet ( $g_{\parallel} > g_{\perp} > 2.0$ ).<sup>23</sup> The spectrum of **2** in a 7:3 methanol:toluene (v/v) glass (80 K) is displayed in Figure 6a. Interestingly, the EPR spectra of **1–3** are practically identical with very similar  $g_{\parallel}$  (range = 2.222–2.217),  $g_{\perp}$  (range = 2.049–

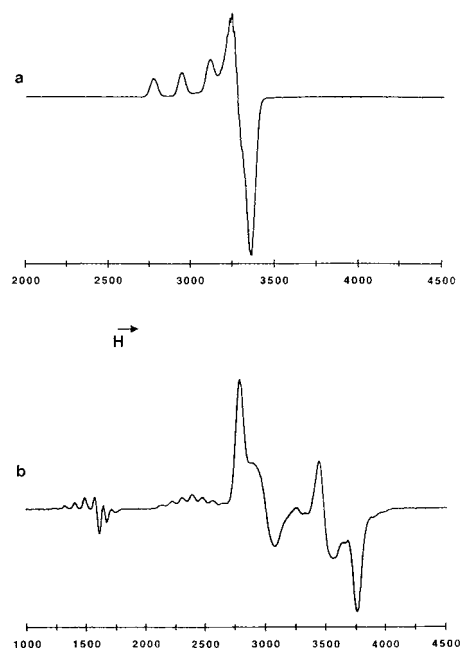


**Figure 6.** X-band EPR spectra of (a)  $[\text{Cu}(\text{Py}_3\text{A})(\text{Cl})]$  (**1**) in 7:3 methanol:toluene (v/v) glass and (b)  $[\text{Cu}(\text{Py}_3\text{A})]_2(\text{ClO}_4)_2$  (**5**) in 8:2 water:glycerol (v/v) glass at 80 K. Spectrometer settings: microwave frequency, 9.43 GHz; microwave power, 13 mW; modulation frequency, 100 kHz; modulation amplitude, 2 G.

2.054), and  $A_{\parallel}$  (171–176 G) values.<sup>24</sup> Such similarities indicate that binding of ROH does not affect the copper(II) center electronically. The interaction between the copper(II) center and the axially bound ROH molecule is clearly weak,<sup>25</sup> and we believe that the axial binding of ROH molecules to the copper(II) center is facilitated and stabilized primarily by intramolecular hydrogen bonding between ROH and the pendant pyridine nitrogen.<sup>26</sup>

Much in contrast to **1–3**, the EPR spectra of **4** and **5** in 7:3 water:glycerol (v/v) are complex but well resolved and clearly demonstrate that both species remain dimeric in aqueous solutions. The spectrum of **5** is displayed in Figure 6b. Such spectrum, typical of weakly coupled dimeric copper(II) complexes, has been reported and analyzed before.<sup>5,27,28</sup> The spectrum is expected to have six features arising from the  $-1 \rightarrow 0$  and  $0 \rightarrow +1$  transitions each with  $x$ ,  $y$ , and  $z$  components. There is a positive feature at 2398 G ( $g = 2.81$ ) showing well resolved seven line hyperfine pattern (peak separation = 88 G) resulting from coupling between the two copper(II) ( $I = 3/2$ ) centers. In addition, there are two positive features at 2790 G ( $g = 2.42$ ) and 3444 G ( $g = 1.96$ ) and inflections at 2998 G ( $g = 2.25$ ) and 3482 G ( $g = 1.94$ ). A poorly resolved feature is identifiable in the region of 4200 G ( $g = 1.62$ ) where hyperfine coupling is barely observed. Finally, the feature at 1470 G ( $g = 4.60$ ) is assigned to a forbidden half-field transition ( $+1 \rightarrow -1$ ) with  $\Delta m_s = \pm 2$ . This signal also exhibits seven

(24) Samples for the EPR measurements were prepared as follows. complex **1**,  $\text{CH}_3\text{CN}/\text{DMF}$  (50:50) glass; complex **2**, methanol/toluene (70:30) glass; complex **3**, ethanol/toluene (70:30) glass.

(25) Strong axial coordination lowers  $A_{\parallel}$  values. See: Miyoshi, K.; Tanaka, H.; Kimura, E.; Tsuboyama, S.; Murata, S.; Shimizu, H.; Ishizu, K. *Inorg. Chim. Acta* **1983**, *78*, 23.

(26) This is further supported by the fact that one can recrystallize complex **1** from solvents such as  $\text{CH}_3\text{CN}$ , DMF, NMF, and acetone without any adduct formation.

(27) Jeffery, J. C.; Schatz, E.; Ward, M. D. *J. Chem. Soc., Dalton Trans.* **1992**, 1921.

(28) Maher, J. P.; Rieger, P. H.; Thornton, P.; Ward, M. D. *J. Chem. Soc., Dalton Trans.* **1992**, 3353.

(23) Hathaway, B. J. In *Comprehensive Coordination Chemistry*; Wilkinson, G., Gillard, R. D., McCleverty, J. A., Eds.; Pergamon Press: Oxford, U.K., 1987; Vol. 5, p 668.

lines and peak separation of 88 G. The fact that both **4** and **5** exhibit identical EPR signals indicates that, in aqueous solution, both complexes lose axial interactions with the anion ( $\text{Cl}^-$  and  $\text{ClO}_4^-$ , respectively) and the axial sites are most possibly occupied by water. The magnetic properties of **4** and **5** are currently under study, and the results will be reported at a later time along with other similar dimeric copper(II) complexes.

**Acknowledgment.** Financial support from a grant from the NSF (CHE-9818492) is gratefully acknowledged. The Bruker

SMART 1000 diffractometer was funded in part by NSF Instrumentation Grant CHE-9808259.

**Supporting Information Available:** Illustrations of stacking of  $[\text{Cu}(\text{Py}_3\text{A})(\text{Cl})]$  units in the structure of **1** (Figure S1) and arrangement of lattice water molecules in the structure of  $\mathbf{4}\cdot 8\text{H}_2\text{O}$  (Figure S2) and the X-ray crystallographic files (in CIF format) and tables for the structure determination of **1–5**. This material is available free of charge via the Internet at <http://pubs.acs.org>.

IC000471M